Mon. Not. R. astr. Soc. (1969) **143**, 189–208.

STAR FORMATION IN CLOUDS OF SOLID HYDROGEN GRAINS

V. C. Reddish and N. C. Wickramasinghe

(Received 1968 October 11)

SUMMARY

It is shown that the condensation of hydrogen onto interstellar grains produces a cellular pressure structure in interstellar clouds leading to fragmentation and star formation. The masses of the stars depend on both the gas density and grain abundance. These quantities are calculated for models beginning with a low density and low grain abundance, and in which more grains are produced in late type stars from carbon synthesized in earlier stellar generations.

It turns out that in all cases, supermassive objects are formed first. As the density and opacity of the interstellar clouds increase, the masses of the objects decline. As they pass through the mass range of supernovae, there is an outburst of heavy element production followed by the formation of large numbers of dwarf stars over a prolonged period of time. By that time the helium abundance has reached several per cent. Present values of heavy element and grain abundances are obtained if the mass ejected by supernovae contains on average 4·4 per cent heavy elements, and if 23 per cent of the carbon in late-type stars is ejected in the form of graphite grains. The heavy element abundance averaged over all stars is about a fifth of the solar value.

1. INTRODUCTION

The formation of stars in clouds of atomic hydrogen, by fragmentation and contraction, involves several problems which are difficult to resolve. For an interstellar cloud of $\sim 10^4\, M_\odot$, such as would form a stellar association, a density $n_H \sim 10^8$ cm^{-3} is required for fragmentation into stellar masses (**1**). The observations, however, indicate that fragmentation occurs at densities $\sim 10^3$–10^4 cm^{-3} which is about the density at which the cloud (if it is gaseous) is able to contract as a whole.

Many OB stars are embedded in circumstellar dust clouds (**2**) which are probably the remnants of clouds from which stars have condensed. Such associations are known to be conspicuously deficient in Hα emission, indicating an absence of neutral hydrogen. We have argued (**3**), on the basis of the available data, that the 'missing' hydrogen may be condensed onto graphite grains as solid H_2, and that this may have important consequences for star formation and the evolution of galaxies (**7**), (**12**).

The processes leading to the formation of molecular and solid H_2 in dense interstellar clouds have recently been considered in more detail (**8**). It appears that the hydrogen would freeze down most readily if it is already largely molecular and the grain temperatures are of $\sim 3{\cdot}4$ °K (**7**), (**8**). At densities 10^3–10^4 cm^{-3} the conversion of atomic to molecular hydrogen takes place at grain surfaces in $\sim 10^5$ years, provided the grain temperature is less than $\sim 6{\cdot}5$ °K. Observational data on the 21-cm line in dark clouds indicate that a marked decline in the neutral hydrogen relative to dust begins at points in the cloud where the extinction at 5000 Å exceeds $\sim 1{\cdot}5$ mag (**4**)–(**6**). This data has been interpreted (**8**) to imply that $\tau_v \approx 1{\cdot}5$ mag represents the extinction necessary to lower the grain temperatures to $\sim 6{\cdot}5$ °K—the critical value for H_2 recombination. It then follows that grain temperatures

~ 3–4 °K would occur deeper in the cloud where the optical depth exceeds ~ 3–4 mag. We thus conclude that solid hydrogen condenses onto grains in any cloud which has an opacity at visible wavelengths exceeding ~ 4 mag.

If the extinction within a cloud is $\gtrsim 2$ mag we may assume that solid hydrogen freezes down on the grains leaving only the helium in gaseous form. With $n_{\mathrm{H}_e}/n_{\mathrm{H}} \sim 0{\cdot}1$ in the original cloud, the gas pressure then falls by a factor ~ 10. Furthermore the bulk of the cloud material becomes effectively decoupled from any magnetic field that may be present. Cloud contraction and star formation then readily take place, provided there is no angular momentum. The presence of even a modest amount of angular momentum would have the effect of halting the contraction at a stage when the rotational energy became comparable with the gravitational energy. For the purposes of the present paper we shall assume that most of the angular momentum of a contracting cloud fragment is removed through magnetic coupling with the interstellar medium, before solid hydrogen is able to form. This transference of angular momentum then occurs during the stage when the gas density rises from the mean interstellar value ~ 1 cm^{-3} to $\sim 10^4$ cm^{-3} which appears to be appropriate to cloud complexes such as those in Cygnus (**1**). Any angular momentum which is retained at the stage when the gas density rises to $\sim 10^4$ cm^{-3} must be removed by processes other than magnetic coupling. A more detailed study of the angular momentum question is outside the scope of the present discussion.

In view of the preceding remarks we consider it reasonable to postulate that the formation of solid hydrogen grains is a necessary condition for the formation of stars, and possibly of galaxies also. It has already been pointed out (**7**) that several astrophysical phenomena may be accounted for on the basis of this hypothesis. The negative feedback inherent in the loop:

Grain cooling → solid hydrogen condensation → star formation → grain heating

establishes and maintains equality between the energy densities of the microwave background, starlight, and the energy released by the synthesis of the cosmic helium abundance from hydrogen. It accounts further for the observed constancy of the rate of star formation per unit mass of interstellar gas among galaxies (**12**), since the background temperature is maintained close to the critical value of ~ 3 °K.

In the present communication we propose to investigate the evolution with time of several galactic quantities such as the ratio of graphite grains to gas, the helium and heavy element abundances and the average stellar mass.

2. CONDENSATION OF SOLID HYDROGEN

The rate of condensation of solid hydrogen may be computed as a function of the grain temperature T_{g}. The number of hydrogen atoms striking a grain of radius a per second, is:

$$\sim 4\pi a^2 n_{\mathrm{H}} (kT_{\mathrm{kin}}/2\pi m_{\mathrm{H}})^{1/2} \tag{1}$$

where T_{kin} is the gas kinetic temperature. The rate at which H_2 molecules leave the surface is

$$\sim \alpha 4\pi a^2 . \frac{p_{\mathrm{sat}}}{kT_{\mathrm{g}}} (kT_{\mathrm{g}}/4\pi m_{\mathrm{H}})^{1/2} \tag{2}$$

where T_{g} is the grain temperature and p_{sat} is the saturation vapour pressure of solid hydrogen. With $\alpha \sim 0{\cdot}1$ the net rate of increase of mass is

$$\frac{dm_{\mathrm{SH}}}{dt} \simeq 4\pi a^2 n_{\mathrm{H}} \left(\frac{kT_{\mathrm{kin}}}{2\pi m_{\mathrm{H}}}\right)^{1/2} . m_{\mathrm{H}} - 4\pi a^2 . \frac{p_{\mathrm{sat}}}{kT_{\mathrm{g}}} . \left(\frac{kT_{\mathrm{g}}}{4\pi m_{\mathrm{H}}}\right)^{1/2} . 2m_{\mathrm{H}}. \tag{3}$$

Equating (3) to $4\pi a^2 s\, da/dt$ we have for the rate of increase of grain radius:

$$\frac{da}{dt} = s^{-1}\left(\frac{km_{\mathrm{H}}}{2\pi}\right)^{1/2}\left[n_{\mathrm{H}}T_{\mathrm{kin}}{}^{1/2} - \frac{\sqrt{(2)}\cdot p_{\mathrm{sat}}}{kT_{\mathrm{g}}{}^{1/2}}\right] \tag{4}$$

where s is the density of solid H_2, $\sim 0{\cdot}1$ g cm^{-3}. The saturation vapour pressure of solid hydrogen p_{sat} may be calculated as a function of T_{g} assuming a sublimation energy (7) ~ 260 cal mol^{-1}. With $T_{\mathrm{kin}} = 10^2$°K, $n_{\mathrm{H}} \approx 10^4$ the value of da/dt was calculated from equation (4) and is tabulated in Table I as a function of T_{g}.

TABLE I

T_{g}(°K)	da/dt (cm s^{-1})	Time to grow to $a = 10^{-4}$ cm (s)	$n_{\mathrm{H}}{}^1$ cm^{-3} after $1{\cdot}5 \times 10^{11}$ s	p/p_0 after $1{\cdot}5 \times 10^{11}$ s
3·388	$-0{\cdot}47 \times 10^{-15}$		10^4	1
3·386	$-0{\cdot}32 \times 10^{-15}$		10^4	1
3·384	$-0{\cdot}16 \times 10^{-15}$		10^4	1
3·382	$-0{\cdot}16 \times 10^{-16}$		$\sim 10^4$	1
3·380	$0{\cdot}13 \times 10^{-15}$	$0{\cdot}78 \times 10^{12}$	$9{\cdot}93 \times 10^3$	0·99
3·378	$0{\cdot}27 \times 10^{-15}$	$0{\cdot}37 \times 10^{12}$	$9{\cdot}36 \times 10^3$	0·94
3·376	$0{\cdot}41 \times 10^{-15}$	$0{\cdot}24 \times 10^{12}$	$7{\cdot}6 \times 10^3$	0·78
3·374	$0{\cdot}54 \times 10^{-15}$	$0{\cdot}18 \times 10^{12}$	$4{\cdot}7 \times 10^3$	0·52
3·372	$0{\cdot}68 \times 10^{-15}$	$0{\cdot}15 \times 10^{12}$	$\sim$ 0	0·09
3·370	$0{\cdot}81 \times 10^{-15}$	$0{\cdot}12 \times 10^{12}$	$\sim$ 0	0·09
3·368	$0{\cdot}93 \times 10^{-15}$	$0{\cdot}11 \times 10^{12}$	$\sim$ 0	0·09

With a grain/H ratio of $\sim 10^{-12}$ the maximum size of a hydrogen grain is $\sim 10^{-4}$ cm—about 10 times the original radius of a graphite-ice grain. In the third column of Table I we have set out the time required for growth to this maximum radius. All these times scales are comparable with the gravitational collapse times at densities 10^3–10^4 cm^{-3}.

Within a specified time interval Δt suppose that an average of x atoms of hydrogen have stuck on each grain, in a particular region. The ambient number density of H atoms is then reduced to

$$n_{\mathrm{H}}{}^1 = n_{\mathrm{H}} - x n_{\mathrm{g}}.$$

Since the quantity x is related to the grain radius a by

$$x = \tfrac{4}{3}\pi a^3 \frac{s}{m_{\mathrm{H}}}$$

we have

$$n_{\mathrm{H}}{}^1 = n_{\mathrm{H}} - \tfrac{4}{3}\pi a^3 \frac{s}{m_{\mathrm{H}}} n_{\mathrm{g}}. \tag{5}$$

Here a is given by the second column of Table I for the specified Δt, at various grain temperatures. If the time interval considered is $\Delta t \sim 1{\cdot}5 \times 10^{11}$ s, the number density $n_{\mathrm{H}}{}^1$ as a function of T_{g} is given in the fourth column of Table I. (Here $n_{\mathrm{g}}/n_{\mathrm{H}} = 10^{-12}$, $n_{\mathrm{H}} = 10^4$ cm^{-3} is assumed). In the fifth column of the table is given the gas pressure, the sum of the partial pressures of hydrogen, helium and grains, relative to that before condensation of the hydrogen took place (assuming $n_{\mathrm{H}_e}/n_{\mathrm{H}} = 0{\cdot}1$). The extreme sensitivity of the residual hydrogen density and pressure to the grain temperature is evident in Table I.

Throughout the preceding argument it was assumed that essentially all the ambient H_2 could be mopped up by the grains if its partial pressure exceeded the

vapour pressure of solid H_2. Consider a graphite grain at 3·37 °K in a cloud of molecular hydrogen of density 10^4 cm^{-3}. The vapour pressure of solid H_2 at this temperature corresponds to a number density of $\sim 10^3$ cm^{-3}. Accretion of solid hydrogen by the grain would proceed quite readily until the ambient gas density is reduced to this value. Further condensation will not take place unless the grain temperature has fallen substantially below 3·37 °K. This is indeed likely to occur. The accretion of sufficient H_2 to reduce the gas density from 10^4–10^3 cm^{-3} would have the effect of lowering the grain temperature due to (a) the reduced optical absorption efficiency of the hydrogen coated grain, and (b) the increased infrared emissivity of the larger particle. If the grain temperature is lowered to 2·7 °K, the vapour pressure of solid H_2 is reduced to ~ 10 cm^{-3} or less. Thus the numbers in the last two columns of Table I would be approximately valid, provided T_g is interpreted as the *initial* grain temperature.

In regions of the cloud where T_g is lower, condensation will proceed more quickly and the number density of free atoms and hence the gas pressure will fall more quickly. This process is cumulative, since the growth of a solid hydrogen mantle will (a) enhance the grain's infrared emissivity and (b) increase the total optical depth in the visible—thus enhancing the shielding of external radiation. Both these effects will lower the grain temperatures still further in the condensing regions. The pressure distribution will soon take on a cellular structure, and the cloud will fragment.

The origin of this process of instability differs somewhat from that considered by Field (**22**) and by Pikelner (**23**), in which the variations in density ρ necessary to restore the balance of pressures, $p = \rho\mathcal{R}T/\mu$, are the result of variations in T, the molecular weight μ remaining constant; the variations in T are caused by the dependence of the energy gains and losses on the temperature and density of the gas. In the case of the formation of solid hydrogen grains, the instability is initiated by the large change in number density, and hence in mean molecular weight, resulting from the freezing of the atoms on to the grains. This is accompanied by a lowering of the kinetic temperature due to collisions between atoms and grains, and decoupling of the magnetic field as the ionization level falls (the collision cross-section per unit volume of hydrogen, to cosmic and far ultraviolet radiation, being reduced by the factor $(n_g/n_H)^{1/3} \approx 10^{-4}$). With $n_{H_e}/n_H \leqslant 0{\cdot}1$, the pressure drop initiated in the cooler clouds in this case is greater by one or more orders of magnitude than in the case cited, and this makes possible the formation and contraction of cloud fragments of much smaller mass from a given initial density. This overcomes the difficulty, referred to in the Introduction, that the data on the mean densities of clouds in which stars form indicates that they are much too low for contraction of fragments of stellar mass, if the hydrogen is atomic or molecular.

3. FRAGMENTATION AND STAR FORMATION

The characteristic dimension l of a fragment will be determined by the distance over which the grain temperature of graphite–ice grains remains uniform to $\sim 10^{-2}$ °K to 10^{-3} °K as the grain temperature falls. This will be of order unit optical depth or greater. It will not, however, be so large as the optical depth required to shield the grains from external radiation sufficiently for T_g to fall to the temperature at which the hydrogen condenses, which is $\tau \gtrsim 4$. We have therefore chosen $\tau \approx 2$ as the characteristic dimension of the cellular pressure structure which leads to the

fragmentation. Hence

$$\pi a^2 Q_{\text{ext}} n_g l \sim 2 \tag{6}$$

where Q_{ext} is the extinction efficiency of a graphite–ice grain at optical wavelengths and n_g is the number density of grains. The mass of a spherical fragment of diameter l is given by

$$M_f \approx 1{\cdot}6 \times 10^{-58} a^{-6} Q_{\text{ext}}^{-3} \left(\frac{n_g}{n_H}\right)^{-3} n_H^{-2} \text{ solar masses.} \tag{7}$$

With $a \approx 1{\cdot}5 \times 10^{-5}$ cm, $Q_{\text{ext}} \approx 1{\cdot}5$, $n_H \approx 5 \times 10^3$ cm^{-3}, $n_g/n_H \sim 10^{-12}$ we have $M_f \sim 0{\cdot}20\, M_\odot$—which is close to the value $\sim 0{\cdot}11 M_\odot$ derived from the mass density in the galactic plane (**13**).

The condensation of all the hydrogen onto grains will increase the average grain radius by a factor ~ 10 and the optical extinction in the fragment by $\sim 10^2$. The optical depth of the fragment at millimeter wavelengths will then certainly rise above unity and the cloud as a whole will be able to radiate away the thermal energy released through gravitational contraction—thereby maintaining the H_e gas at ~ 3 °K.

In the above discussion it was assumed that the cloud fragment at a temperature ~ 3 °K would be unstable towards gravitational collapse. The condition for collapse is

$$\frac{3}{5}\frac{GM}{R} > \frac{3\mathscr{R}T}{\mu}$$

i.e.

$$\frac{M}{R} > \frac{5\mathscr{R}}{G}\frac{T}{\mu}. \tag{8}$$

With $T = 3$ °K (for all temperatures) the right hand of equation (8) has the value $1{\cdot}9 \times 10^{15}$. The cell is now compressed to a radius $\sim 10^{17}$ cm and has a density $\sim 1{\cdot}6 \times 10^{-19}$ g cm^{-3}; M/R is thus $\sim 6{\cdot}7 \times 10^{15}$. Since equation (8) is satisfied contraction is able to proceed.

An interesting phenomenon arises when some of the fragments have contracted to form stars. The radiation from these stars will evaporate any remaining solid hydrogen grains in their immediate vicinity (within ~ 1 pc)and as a result the gas pressure there will rise by a factor ~ 10 (assuming initially $n_H/n_{H_e} \sim 10$ and that there has been no diffusion). The time scale for evaporation is very short, $< 10^{10}$ s, compared with the time for a sound wave to travel a distance ~ 1 pc. Explosive expansions of the evaporated regions will consequently take place. Regions between evaporated domains will be compressed and this may lead to further star formation. If the helium diffuses out of the clouds of solid hydrogen grains before evaporation, the increase in gas pressure subsequent to evaporation will be by a factor $\sim 10^{12}$. The possibility arises, in this case, that compression of clouds of diffused helium may produce pure helium stars (we are indebted to F. Hoyle for drawing our attention to this latter possibility).

It is of interest in the present context that 21-cm observations (**10**) have indeed revealed the presence of expanding shells of atomic hydrogen around some stellar associations. Cugnon (**11**) has also drawn attention to a similar 21-cm feature which is also probably associated with a stellar association.

4. EVOLUTION OF A GALAXY

Throughout the preceding discussion we confined our attention to the case of star formations under present day galactic condition: $n_H \simeq 10^4$, $n_g/n_H \sim 10^{-12}$. We shall now consider star formation under more general conditions and also examine its relationship to some features of the evolution of a galaxy as a whole.

For general values of the parameters n_H, n_g/n_H the average stellar mass is given essentially by equation (7):

$$\bar{M} = 5 \times 10^{-30} \left(\frac{n_g}{n_H}\right)^{-3} n_H^{-2} \text{ solar masses.} \tag{9}$$

subject to two further conditions:

(a) the condition (6) for gravitational collapse must be satisfied, and

(b) the condensation of all hydrogen onto grains must take place in a permitted time scale.

The requirement (a) is obtained from equations (6), (8) and (9) where a and Q_{ext} occurring in equation (6) refer to the original graphite–ice grain. With $Q = 1{\cdot}5$, $a = 1{\cdot}5 \times 10^{-5}$ cm, $T \cong 3\,^{\circ}$K these yield

$$\left(\frac{n_g}{n_H}\right)^2 n_H \leqslant 2{\cdot}10^{-21}. \tag{10}$$

For a grain–gas ratio n_g/n_H the final radius of a hydrogen mantle is

$$r = \left(\frac{3}{4\pi} \frac{m_H . n_H}{s . n_g}\right)^{1/3}. \tag{11}$$

The time scale t_{SH} for growth to this radius is given by equation (4) where the second term on the R.H.S. is neglected:

$$t_{SH} = s \left(\frac{kTm_H}{2\pi}\right)^{-1/2} \left(\frac{3m_H}{4\pi s}\right)^{1/3} n_H^{-1} \left(\frac{n_g}{n_H}\right)^{-1/3}$$

$$\simeq 3{\cdot}4 \times 10^{11} n_H^{-1} \left(\frac{n_g}{n_H}\right)^{-1/3}. \tag{12}$$

Equations (10) and (12) enable us to make some estimate of the values of n_H to be used in equation (9).

From equation (10),

$$\log n_H \leqslant -2 \log (n_g/n_H) - 20{\cdot}7 \tag{13}$$

and this relationship is shown on Fig. 1 as a solid line marked (a). The hatched area is thus forbidden for star formation because the condition for gravitational contraction of the cloud fragments is not satisfied within it.

Re-writing equation (12)

$$\log n_H \geqslant -(1/3) \log (n_g/n_H) - \log t_{SH} + 11{\cdot}53 \tag{14}$$

as the condition for growth of solid hydrogen grains, we now enquire as to the value of t_{SH}.

In the first instance, before stars have formed in the galaxy, the time available is a moderate fraction of the Hubble time, say 10^{17} s. That is to say, hydrogen particles will grow as soon as the density has increased by contraction of the protogalaxy cloud sufficiently for grains to grow in the time available. Thus

$$\log n_H \geqslant -1/3 \log (n_g/n_H) - 5{\cdot}47. \tag{15}$$

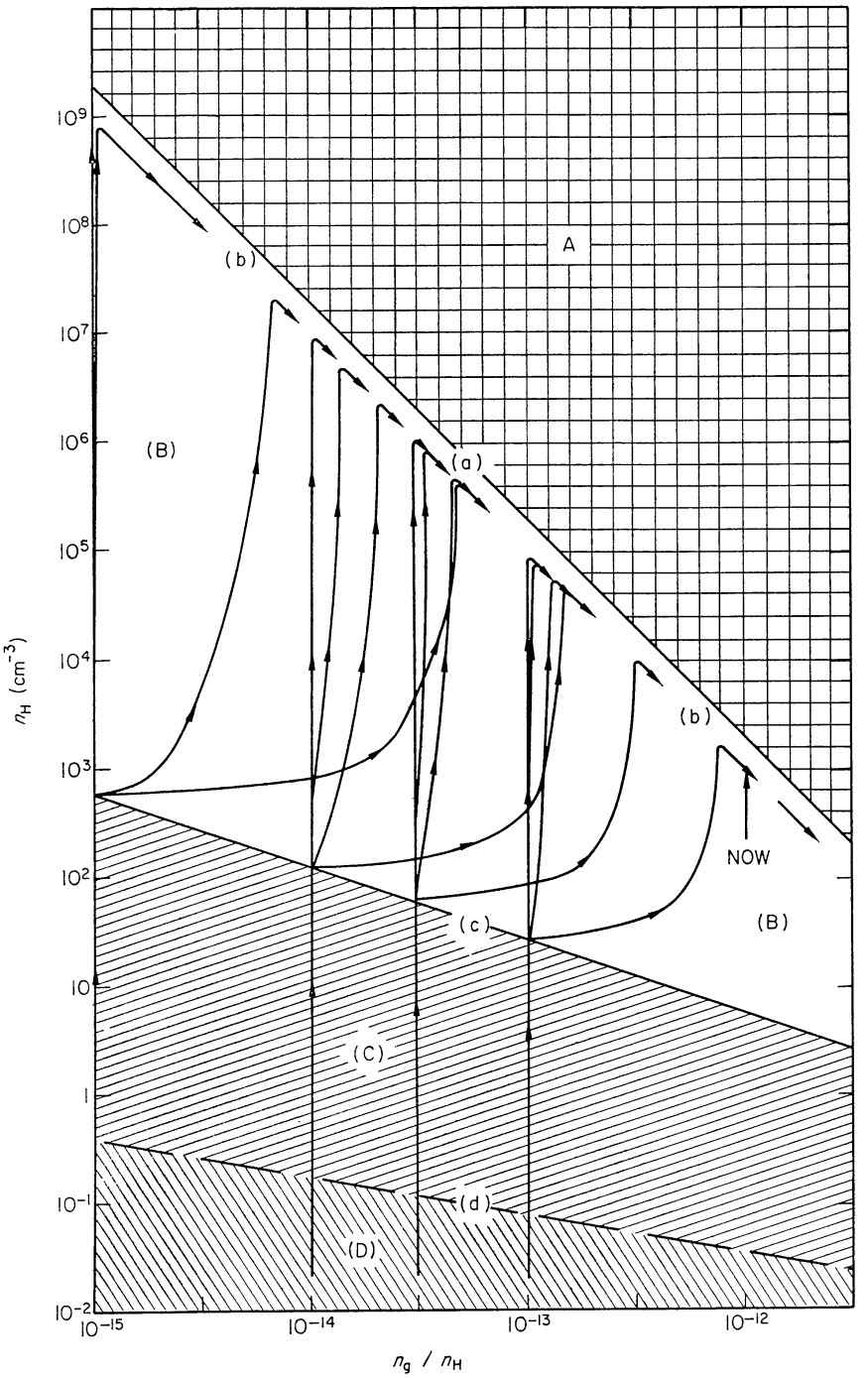

FIG. 1. *Gas density against grain abundance in interstellar clouds. The evolutionary tracks of clouds which form stars are shown by the arrowed lines. The shaded areas are forbidden regions—see text. For each starting value of* n_g/n_H, *the four tracks are (from left to right) for* $R = 1, 10^{-1}, 10^{-2}$ *and* 10^{-3} *respectively, where R is the ratio of the rate of contraction of the clouds to the gravitational free fall rate.*

This is shown as a broken line marked (d) on Fig. 1. Below it the density is too low for solid hydrogen grains to grow in a cosmic time scale. Above it, solid hydrogen grains will grow; but if the time scale for their growth is larger than that for gravitational contraction, fragmentation as described in Sections 2 and 3 will not

occur. The time scale for gravitational contraction is

$$t_G = 1{\cdot}4 \times 10^{15} n_H^{-1/2} \tag{16}$$

and thus the condition for fragmentation of clouds of solid hydrogen grains, $t_{SH} < t_G$, gives

$$\log n_H \geqslant -(2/3) \log (n_g/n_H) - 7{\cdot}25. \tag{17}$$

This relationship is shown as the line marked (c) on Fig. 1. In the area between lines (c) and (d) grains of solid hydrogen grow but not quickly enough for the cellular pressure distribution to develop before the cloud has contracted to the boundary (c). The region (B) between (a) and (c) is that where star formation proceeds.

The evolution of the clouds from which stars form may now be described with reference to Fig. 1. Starting with a given abundance n_g/n_H of ice–graphite grains, the density increases at constant grain abundance as the clouds contract.

At (c), fragmentation and star formation begins. The more massive stars produce heavy elements including carbon, and eject it into the interstellar gas by supernovae explosions. Later generations of stars formed from this gas process the carbon into graphite grains during the red giant stage of their evolution, and these are ejected into interstellar clouds. Thus the grain abundance rises, and the evolutionary track of the contracting clouds moves to the right as well as upwards.

It is to be expected that the most dense clouds will be the coldest and therefore solid hydrogen grain and star formation will proceed most quickly in them. Clouds may contract to higher densities than the line (a) but they fragment into masses too small to undergo gravitational contraction and in time will be re-dispersed into the diffuse interstellar gas. Consequently as the grain abundance increases, star formation proceeds in clouds with densities just below the boundary (a).

The boundary (a) applies to the minimum stellar mass M_1; the average stellar mass is $\bar{M} = 4M_1$ (see Section 5) and consequently when we use equation (9) we employ a value of n_H lower by a factor two than set by the equality sign in equation (13), and this is shown by the line (b) on Fig. 1.

When star formation starts at boundary (c) on Fig. 1, the heating of the gas clouds by the stars may reduce the rate of contraction from (c) to (b). Therefore in the results to be described, calculations have been made for rates of contraction equal to the gravitational free fall rate and for rates slower by factors of 10, 10^2 and 10^3. Thus from (c) to (b) the gas density varies with time according to

$$dn_H/dt = 3{\cdot}35 \times 10^{-16} R n_H^{3/2} \text{ s}^{-1} \tag{18}$$

where $R = 1$ for gravitational free-fall.

In order to calculate the track of evolution of the clouds on Fig. 1, we have to determine the rate of production of interstellar graphite grains.

5. RATES OF STAR FORMATION, PRODUCTION OF HEAVY ELEMENTS AND GRAINS

We have already pointed out that the solid hydrogen hypothesis will tend to maintain an overall constancy in the rate of star formation per unit mass of interstellar gas (**7**), (**12**). This rate will be such that the energy released by the conversion of hydrogen to helium in stars just maintains the energy loss through universal

expansion. Evidence from star counts giving the rate of star formation in the local group of galaxies suggests that the rate of condensation of mass into stars is (**13**)

$$\frac{dM_{\text{stars}}}{dt} = -\frac{dM_{\text{gas}}}{dt} = 1{\cdot}3 \times 10^{-17} M_{\text{gas}} \text{ g s}^{-1} \tag{19}$$

where M_{stars} and M_{gas} represents respectively the masses of stars and of interstellar gas.

The distribution function of stellar masses at formation is known, from evidence in our Galaxy, to be (**1**):

$$F(M) \propto M^{-7/3}; \quad M_1 \leqslant M \leqslant M_2 \tag{20}$$

where $F(M)\,dM$ is the number of stars formed with masses between M and $M+dM$, M_1 and M_2 are respectively the smallest and largest stellar masses formed. If $M_2 \gg M_1$ it follows from equation (20) that the average mass

$$\bar{M} \cong 4M_1. \tag{21}$$

We next obtain expressions for the rates of change with time of the heavy element abundance Z and of the grain–gas ratio n_g/n_H. We assume that heavy elements are produced and ejected by supernovae explosions of stars (**14**) with masses in the range $30M_\odot$ to $10^3 M_\odot$. We shall make the reasonable assumptions that all the mass of these stars is ejected by the explosion and that the fractions of it in the form of heavy elements, carbon and helium synthesized in them are respectively Z_{SN}, C_{SN} and $Y_{SN}(1-Y)$.

It will turn out in the subsequent calculations that the masses derived by equation (9) close to the limit (c) on Fig. 1, that is at the beginning of fragmentation and condensation of the galactic clouds, correspond to supermassive objects. The transition in terms of mass between a supernova and a supermassive object is not known with certainty; we have taken it to be $10^3 M_\odot$; for masses above this, suffixes SM are used to denote supermassive objects.

The fraction of the mass condensing into stars more massive than $\mu M_\odot$ is

$$f_\mu = \int_{\mu M}^{M_2} F(M) M\,dM \Big/ \int_{M_1}^{M_2} F(M) M\,dM. \tag{22}$$

Taking $M_2 = \infty$, $F(M)$ from equation (20) and using equation (21) we have

$$f_\mu = \left(\frac{\bar{M}}{4\mu}\right)^{1/3}. \tag{23}$$

The enrichment of the interstellar gas by heavy elements in the time interval dt is then

$$dZ = (dM_{\text{stars}}/M_{\text{gas}}).\{Z_{SN}(f_{30} - f_{1000}) + Z_{SM}.f_{1000}\} \tag{24}$$

where dM_{stars} is the amount of mass condensed into stars in the same interval. Using equation (19) this gives

$$dZ/dt = 1{\cdot}3 \times 10^{-17}\{Z_{SN}(.f_{30} - f_{1000}) + Z_{SM}.f_{1000}\}. \tag{25}$$

Similarly for the carbon and helium abundances

$$dC/dt = 1{\cdot}3 \times 10^{-17}\{C_{SN}(f_{30} - f_{1000}) + C_{SM}.f_{1000}\} \tag{26}$$

and

$$dY/dt = 1{\cdot}3 \times 10^{-17}\{Y_{SN}(f_{30} - f_{1000}) + Y_{SM}.f_{1000}\}\{1 - Y\}. \tag{27}$$

The interstellar gas contains carbon, and graphite grains. Consequently when a mass M of interstellar gas condenses to form a star it will contain a total mass of carbon

$$\left[C+\left(\frac{n_g}{n_H}\right)\left(\frac{m_g}{m_H}\right).X\right].M \tag{28}$$

where X is the mass fraction of hydrogen in the interstellar gas and m_g is the mass of a graphite grain. With $X\approx 0{\cdot}8$, $m_g\approx 10^{-15}$ g this gives

$$Z_C = C+5{\cdot}10^8\left(\frac{n_g}{n_H}\right) \tag{29}$$

for the carbon abundance in the star.

Graphite grains may be synthesized in the atmospheres of Mira variables and other M-type giants and supergiants (**15**) and in the explosions of supermassive objects (**16**). It is probable that all stars with masses $\geqslant 10M_\odot$ pass through a stage during their evolution in which they synthesize graphite grains from carbon and eject them into the interstellar medium.

If M_{grains} and M_{gas} represent respectively the mass of grains and gas per unit volume

$$\frac{n_g.m_g}{n_H m_H} = \frac{M_{\text{grains}}}{X.M_{\text{gas}}} \tag{30}$$

so that

$$\frac{d}{dt}\left(\frac{n_g}{n_H}\right) = 2{\cdot}10^{-9}\,\frac{d}{dt}\left(\frac{M_{\text{grains}}}{M_{\text{gas}}}\right). \tag{31}$$

The right hand side of equation (31) may be computed in a manner similar to the derivation of equation (25). Thus if F_C is the fraction of the carbon content in stars more massive than $\sim 10M_\odot$ which is ejected in the form of graphite grains, we obtain

$$\frac{d}{dt}\left(\frac{n_g}{n_H}\right) = 2{\cdot}6\times 10^{-26}F_C.f_{10}.Z_C. \tag{32}$$

It should be noted here that equations (25)–(32) were derived with the implicit assumption that for the stars involved here the interval between star formation and the ejection of heavy elements or graphite grains is short compared with the time-scale for the growth of Z and n_g/n_H. Such an assumption would indeed appear valid for the massive stars considered here which have relatively short lifetimes.

6. CALCULATIONS

Equations (9), with (13), (17) and (18) and equations (25)–(29) and (32), may now be solved simultaneously to give

$$\begin{aligned}
\bar{M} &= \bar{M}(t, F_C, C_{SN}, C_{SM})\\
Z &= Z(t, F_C, C_{SN}, C_{SM}, Z_{SN}, Z_{SM})\\
Y &= Y(t, F_C, C_{SN}, C_{SM}, Y_{SN}, Y_{SM})\\
n_g/n_H &= (n_g/n_H)(t, F_C, C_{SN}, C_{SM})\\
n_H &= n_H(t, F_C, C_{SN}, C_{SM}).
\end{aligned}$$

For the composition of matter ejected from supermassive objects (**17**) ($M\geqslant 10^3M_\odot$) we have taken

$$\begin{aligned}
Z_{SM} &= 10^{-5}\\
C_{SM} &= 10^{-4}.
\end{aligned}$$

The helium abundance Y is discussed below.

For the composition of the matter ejected from supernovae ($30 \leqslant M \leqslant 10^3 M_\odot$) we have assumed $C_{SN} = 0{\cdot}16 Z_{SN}$. For the helium abundance we have considered two possibilities, $Y_{SN} = Y_{SM}$ and $Y_{SN} = 0$. This has been done because there is doubt about the amount of helium produced in both kinds of objects and because the mass at which the transition from the one to the other occurs is ill-determined. The two cases may be expected to bracket the true value.

We then applied the condition that the calculations must produce present-day abundances, that is, at $t = 3 \times 10^{17}$ s; $Z = 0{\cdot}02$, $Y = 0{\cdot}3$, $n_g/n_H = 10^{-12}$, and we determined by iteration those values of Z_{SN}, F_C, Y_{SN} and Y_{SM} which are required to satisfy this condition (to within ± 10 per cent).

The claculations were carried out for four different starting values of grain abundance $n_g/n_H(t = 0)$, viz. 10^{-15}, 10^{-14}, 3×10^{-14} and 10^{-13}, and for four different values of the rate of contraction of the gas cloud densities (from (c) to (b) on Fig. 1) as a fraction of the gravitational free fall rate, viz. $R = 1$, 10^{-1}, 10^{-2} and 10^{-3}.

The results of the calculations of n_H, $\bar{M}$, Z, Y and n_g/n_H are displayed graphically in Figs 1–6, and in Table II are given the values of Z_{SN}, F_C, Y_{SN} and Y_{SM} derived for the different values of $n_g/n_H(t = 0)$ and R.

TABLE II

The table gives Z_{SN}, F_C, $Y_{SM}(Y_{SN} = Y_{SM})$ and $Y_{SM}(Y_{SN} = 0)$

n_g/n_H $(t = 0)$;	$R=$ 1	10^{-1}	10^{-2}	10^{-3}
10^{-15}	0·048	0·048	0·045	0·038
	0·30	0·30	0·28	0·21
	0·51	0·48	0·30	0·05
	1·58	1·47	0·87	0·23
10^{-14}	0·042	0·042	0·040	0·041
	0·25	0·25	0·24	0·19
	0·37	0·33	0·14	0·03
	1·31	1·17	0·57	0·12
3.10^{-14}	0·037	0·037	0·038	0·054
	0·22	0·22	0·21	0·17
	0·24	0·20	0·09	0·04
	1·17	1·02	0·46	0·09
10^{-13}	0·032	0·032	0·033	0·10
	0·17	0·17	0·17	0·23
	0·04	0·04	0·03	0·06
	0·98	0·84	0·39	0·07

7. DISCUSSION OF RESULTS

Figs 1–6 show a number of general features which are not strongly dependent on the initial grain abundances $n_g/n_H(t = 0)$ or on the relative contraction rates R. Star formation begins with the formation of supermassive objects.

$$10^7 M_\odot \leqslant M \leqslant 10^{10} M_\odot$$

(Fig. 3) at densities $n_H \sim 10^2$ cm^{-3}, Figs 1 and 2. These eject large amounts of helium and the helium abundance Y rises rapidly with time, Fig. 4. After the first generation they also produce carbon (**17**) (assuming that the helium includes a small proportion of He^3), and the grain abundance n_g/n_H begins to rise slowly, Fig. 6. The

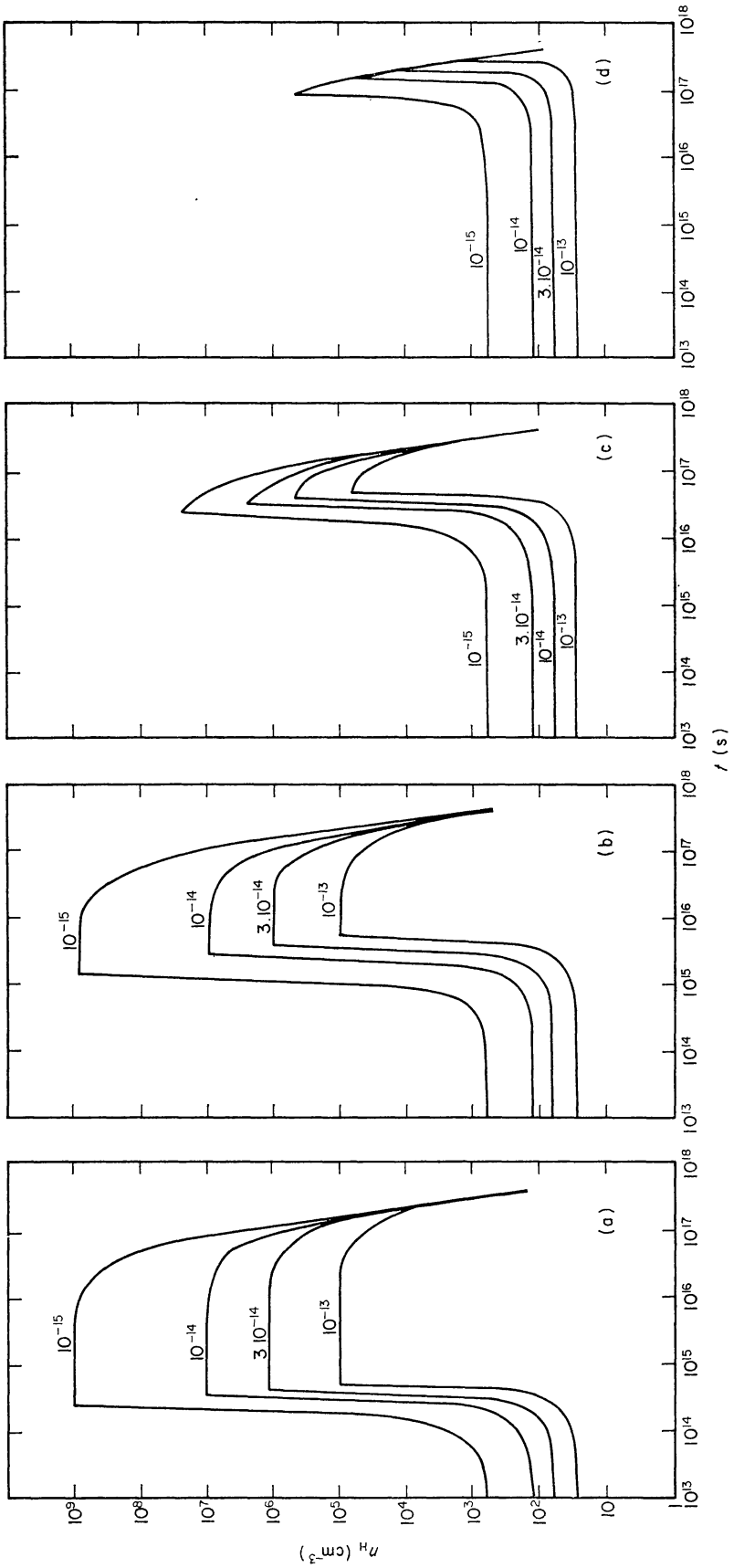

FIG. 2. *Gas density against time, in clouds forming stars. Each curve is marked with the initial grain abundance. (a), (b), (c) and (d) are respectively for values of* $R = 1, 10^{-1}, 10^{-2}, 10^{-3}$.

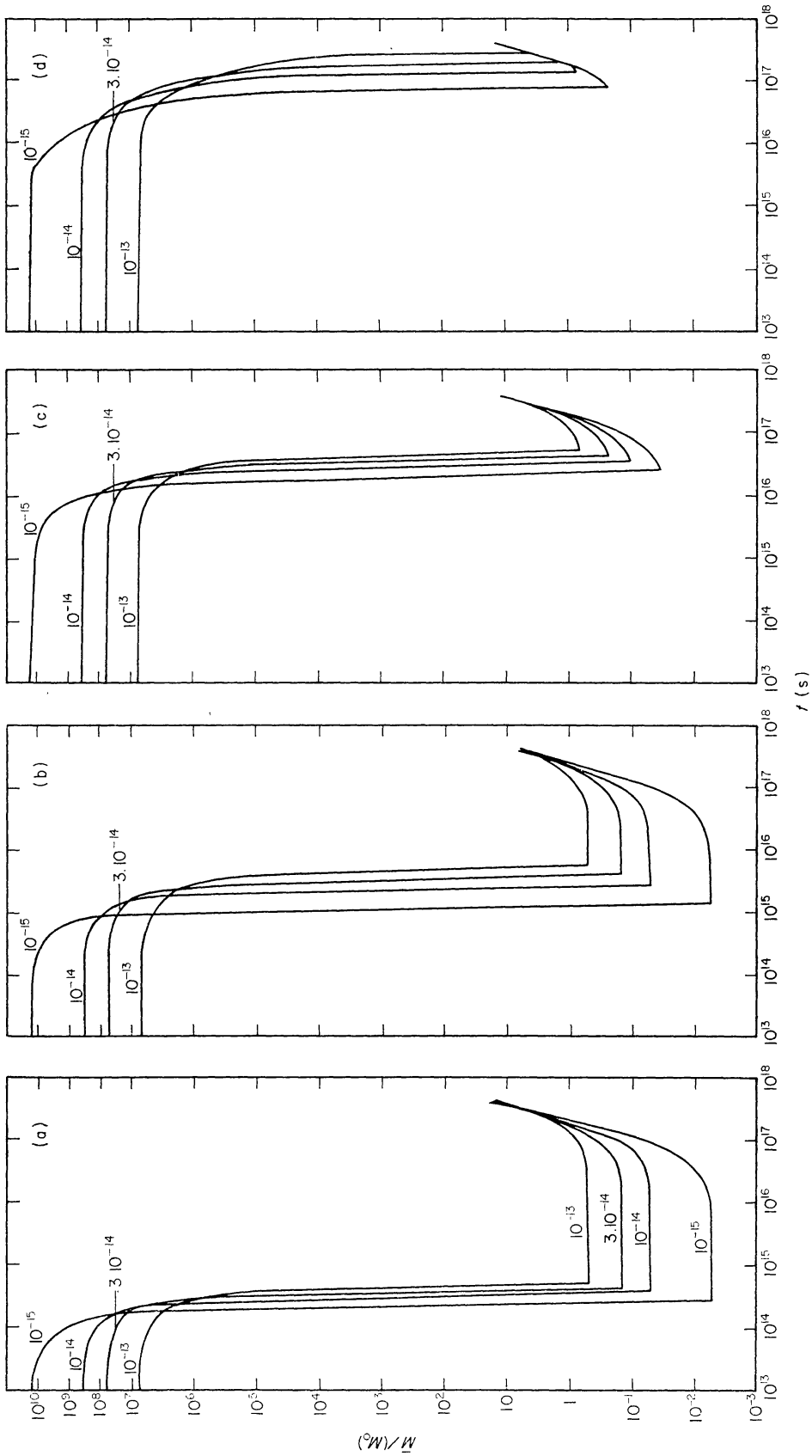

FIG. 3. *Average stellar mass against time. Each curve is marked with the initial grain abundance, (a), (b), (c) and (d) are respectively for values of* $R = 1, 10^{-1}, 10^{-2}, 10^{-3}$.

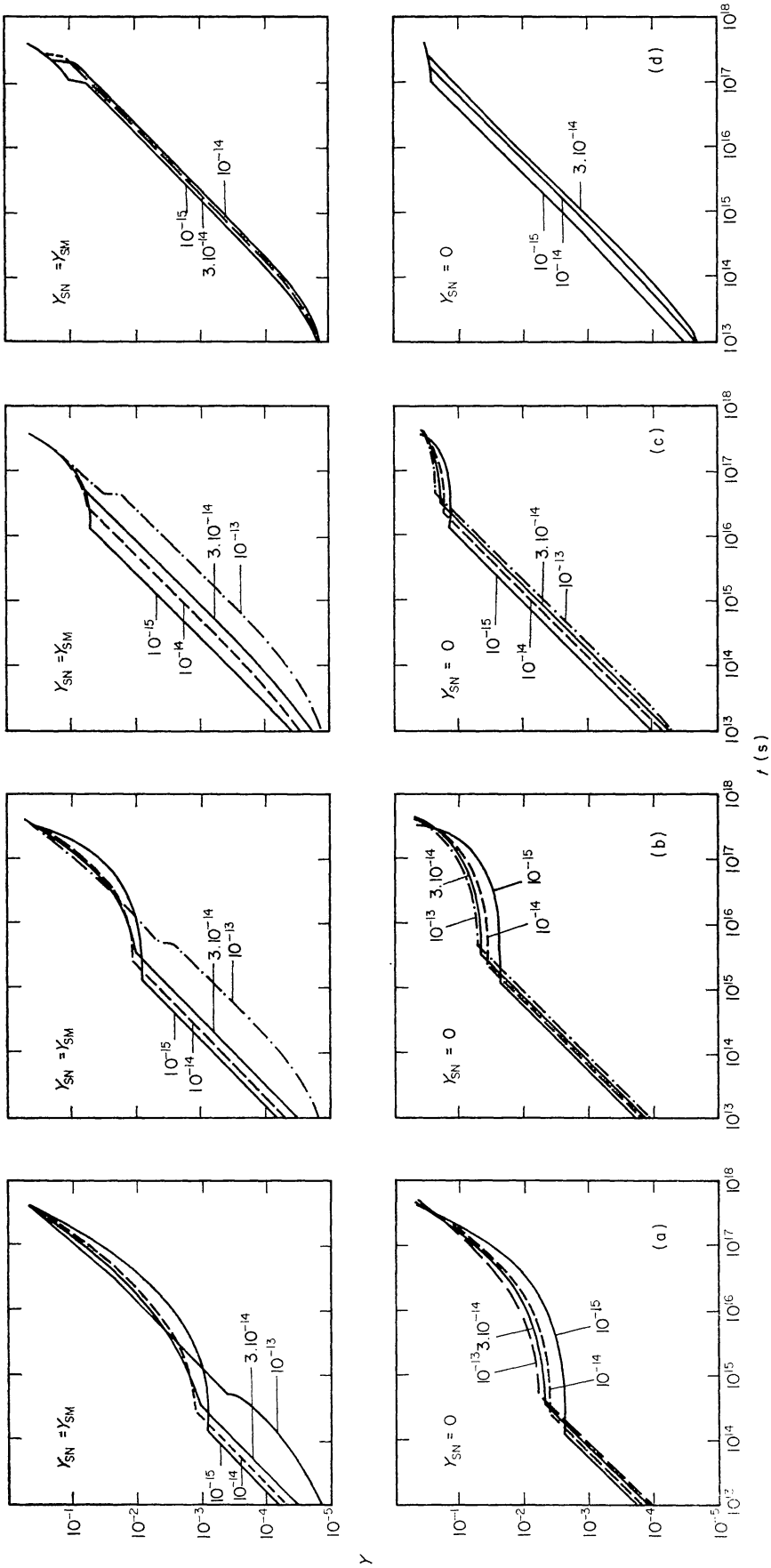

FIG. 4. *Helium abundance against time, for the alternatives $Y_{SN} = Y_{SM}$ and $Y_{SN} = 0$. Each curve is marked with the initial grain abundance. (a), (b), (c) and (d) are respectively for values of $R = 1, 10^{-1}, 10^{-2}, 10^{-3}$.*

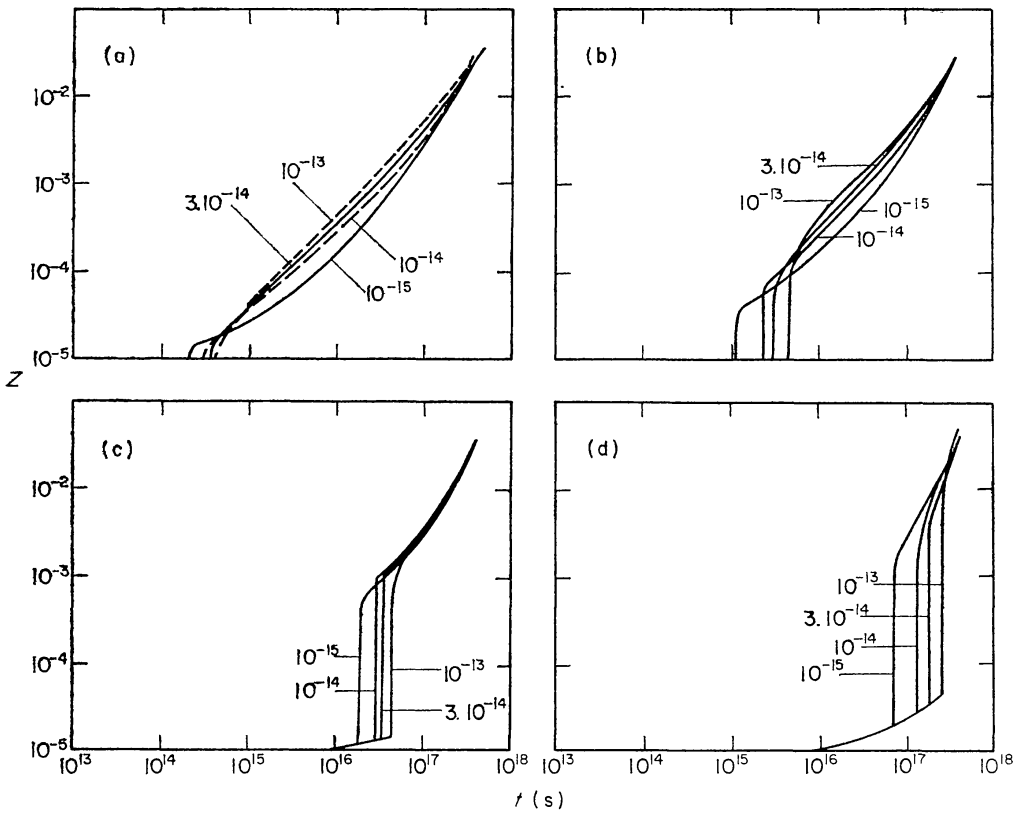

FIG. 5. *Heavy element abundance against time. Each curve is marked with the initial grain abundance.* (*a*), (*b*), (*c*) *and* (*d*) *are respectively for values of* $R = 1, 10^{-1}, 10^{-2}, 10^{-3}$.

density n_H increases as the clouds contract, and both these effects contribute towards increasing the opacity of the clouds and reducing the masses of the cloud fragments. As the average stellar mass falls through the mass range covered by type II supernovae ($30 \leqslant M \leqslant 10^3 M_\odot$), Fig. 3, there is an outburst of production of heavy elements, Fig. 5. The collapse to high densities and high opacities occurs rapidly and thereafter results in the production of large numbers of very dwarf stars, $M \sim 0{\cdot}1 M_\odot$, over a prolonged period of time, Fig. 3. As the ice–graphite grain abundance continues to rise, star formation proceeds in clouds with densities lying along line (b) on Fig. 1 and the average masses of stars formed slowly rises, Fig. 3.

Thus three general and common features of the results, the rapid rise in the helium abundance, the outburst of heavy element synthesis, and the formation of large numbers of dwarf stars, are what appear to be required to account qualitatively for the observational data pertaining to the galaxy and other galaxies (**12**). Before proceeding to a more detailed discussion of these figures we consider the quantities tabulated in Table II.

There was no *a priori* reason for expecting the quantities in the table to be credible—for instance, less than unity.

That they are in fact very reasonable values is evident from a cursory examination of the table, and this indicates that the hypotheses on which this paper is based are not unrealistic.

The abundance of heavy elements in the material ejected by supernovae Z_{SN}, varies little, all but one of the values lying in the range $0{\cdot}031 \leqslant Z_{SN} \leqslant 0{\cdot}054$, with a mean $\bar{Z}_{SN} = 0{\cdot}044$.

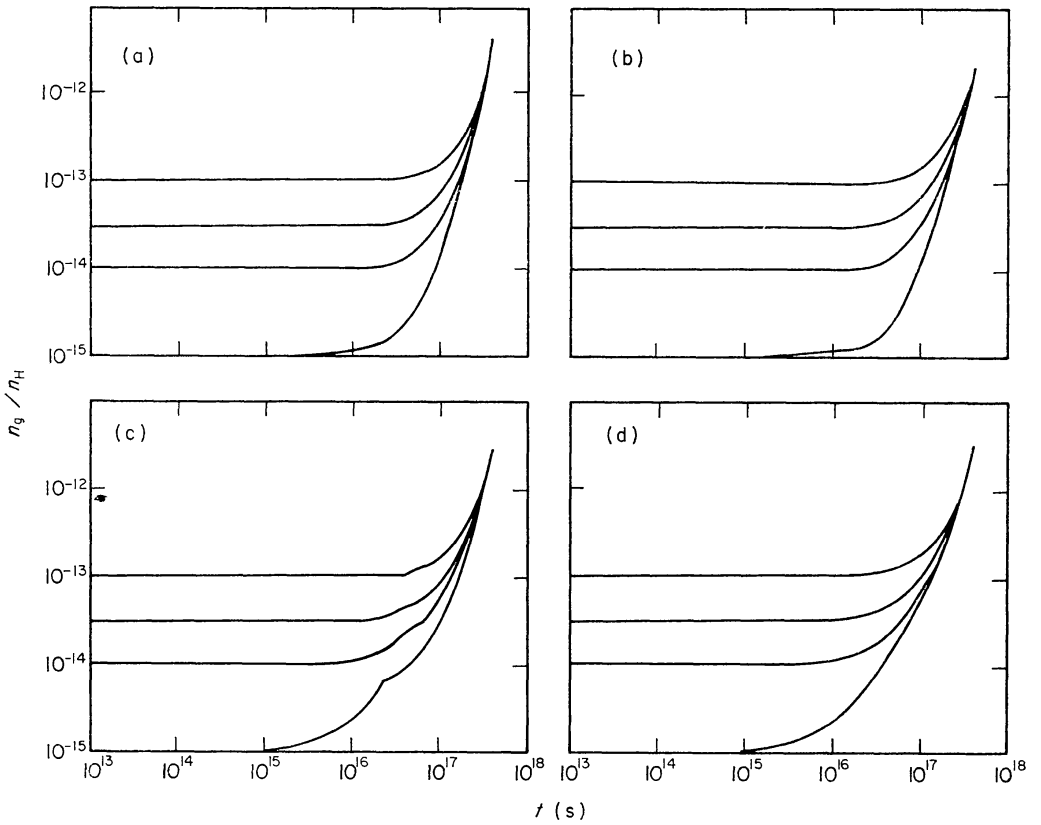

FIG. 6. *Abundance of interstellar graphite grains, against time. Each curve is marked with the initial grain abundance. (a), (b), (c) and (d) are respectively for values of* $R = 1, 10^{-1}, 10^{-2}, 10^{-3}$.

The fraction F_C of the carbon abundance, in stars with masses $\geqslant 10M_\odot$, which is formed into graphite and expelled into the interstellar clouds, lies in the range $0{\cdot}17 \leqslant F_C \leqslant 0{\cdot}31$, with a mean $\bar{F}_C = 0{\cdot}23$.

These values for Z_{SN} and F_C are in good accord with what is to be expected from the physics of the processes involved (**14**)–(**16**). In further development of this work it would be of interest to examine the rate of growth with time of the different heavy elements produced by different processes (**17**), (**18**) but this requires a better knowledge than we have at the present time of the frequency distribution of the masses of the supermassive objects and supernovae which occur and of how the nuclear processes change with the mass.

The values of Y_{SM} and Y_{SN} show a larger variation. We expect Y_{SM} to be $\geqslant 0{\cdot}3$ (**17**) and we can therefore reject those of the combinations of $n_g/n_H(t = 0)$ and R which produce values of Y_{SM} much less than this. These are shown cross-hatched in Table III for the case $Y_{SN} = 0$. Several of the values of Y_{SM} are greater than unity. However, the uncertainties in the values employed in the calculations and the fact that the assumption $Y_{SN} = 0$ is certainly too extreme, do not allow us to regard them as representing unrealistic values of $n_g/n_H(t = 0)$ and R.

If $Y_{SN} = Y_{SM}$, the shaded elements of Table III are also rejected.

An additional limitation may be imposed by the length of time occupied by the supermassive objects and supernovae, Fig. 3. This phase of evolution of the galaxy may be identified with the quasars and Seyfert galaxies, and a limitation of ~ 1 per

TABLE III

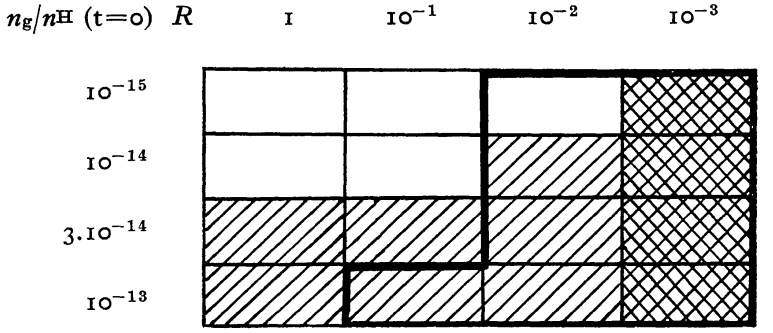

cent on the fraction of all galaxies which are of this kind limits the lifetime of the phase to $\sim 3 \cdot 10^{15}$ s. Applying this to Fig. 3 results in the rejection of those elements of Table III heavily outlined.

We now return to a consideration of the figures, in particular to the growth of the abundances Y and Z subject to the limitations imposed by Table III.

The most rapid rise of helium abundance for $R > 10^{-2}$ occurs when $Y_{SN} = 0$ and $R = 10^{-1}$, Fig. 4(b). By $t \sim 10^8$ yr, Y has reached $2\frac{1}{2}$ to 5 per cent depending on $(n_g/n_H)(t = 0)$, and 10 per cent by $t = 3.10^9$ yr. Two thirds of all the stars now visible would be formed in this time interval, and therefore would have helium abundances in the range given. A third of all stars would have helium abundances greater than 10 per cent. For $R = 10^{-1}$ and $Y_{SN} = Y_{SM}$, the corresponding helium abundances are 1 and 6 per cent. Our knowledge of the distribution of helium abundances among stars is uncertain (**19**) but the results of this paper do not appear to be substantially at variance with what is known.

For all values of $(n_g/n_H)(t = 0)$ and R, the heavy element abundances, Fig. 5, show a rapid rise as the average stellar mass falls through the range of supernovae masses. Thereafter the heavy element abundance rises almost linearly with time and the differences between the various cases are small.

Immediately after the outburst of heavy element production the average stellar mass falls to the lowest value and since the rate of star formation is still very high (see equation (19)), large numbers of dwarf stars will be formed with heavy element abundances equal to and greater than the value following the outburst. In all cases this value is, however, small compared with the present value. Available data indicates that most of the mass in galaxies is in metal-rich dM stars. The growth with time in the number of stars formed may be calculated using equation (9) and (19),

$$N = \int_0^t dN = \int_0^t (1{\cdot}3 \times 10^{-17} M_0/\bar{M}(t)) \exp(-1{\cdot}3 \times 10^{-17} t)\, dt. \tag{33}$$

Taking the lifetime of a main sequence star to be

$$t_{MS} = 3 \times 10^{17} \bar{M}/L \text{ s} \tag{34}$$

where M, L are in solar units, and the mass–luminosity relation

$$L \propto \bar{M}^3 \tag{35}$$

then

$$t_{MS} = 3 \times 10^{17}/\bar{M}^2. \tag{36}$$

Equations (25) and (37) enable the number of stars to be given as a function of heavy element abundance, and this is shown in Fig. 7 for $n_g/n_H(t = 0) = 10^{-14}$, $R = 10^{-1}$, and a total galaxy mass of $10^{10} M_\odot$.

If the Sun was formed at $t = 1{\cdot}5 \times 10^{17}$ s, then from Fig. 5(b) it would have a heavy element abundance equal to 0·3 of the present value (which was taken to be $Z(\text{now}) = 0{\cdot}02$; in view of this result it may be argued that it should have been taken higher. However to a good approximation this would be equivalent to applying a corresponding scaling factor to Z on Fig. 5). It then follows from Fig. 7 that a half of the stars are formed with heavy element abundances greater than one seventh of the solar value, and the average heavy element abundance is about one fifth of the solar value. This is probably lower by a factor 2 to 3 than is indicated by data for stars in the region of the Sun (**20**), and in other galaxies (**21**), but the discrepancy is

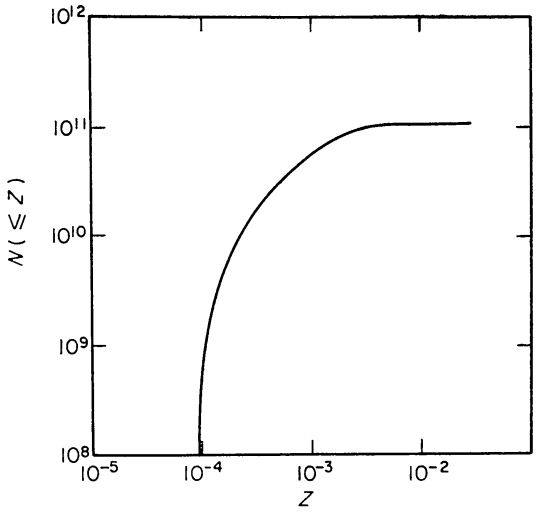

FIG. 7. *Number of stars with heavy element abundances* $\leqslant Z$, *for* $n_g/n_H(t = 0) = 10^{-14}$ *and* $R = 10^{-1}$.

not large compared with the uncertainties in the data. There is the possibility that large numbers of very faint stars with low metal abundances exist which are not included in the data used by Dixon (**20**), and Wood (**21**) points out that his synthesized galaxies contain less mass by a factor three than is indicated by the dynamics of the galaxies. It is evident from Figs 2, 5 and 8 that in the models in this paper a large part of the mass goes into the least massive and hence faintest stars, with the lowest metal abundances.

No marked increase in the rate of growth of Z in the earlier stages of evolution can be achieved by a greater synthesis of heavy elements in supermassive objects. Even if Z_{SM} is raised from 10^{-5} assumed here, to 10^{-3} (which appears to be an upper limit (**17**)) only a small change in the overall growth of Z results, Fig. 8. It appears that the only way in which the heavy element abundances can be raised to a level comparable with the present value, prior to the formation of large numbers of dwarf stars, is for the rate of contraction of the gas to be inhibited (or reversed) at the time of the supernovae outburst. That is to say, n_{H} (Figs 1 and 2) must oscillate about the mean value which in equation (9) produces stars with masses

$$30 \leqslant \bar{M} \leqslant 10^3 M_\odot.$$

Such an oscillation which must evidently result from the outburst of supernovae itself, would result in repeated outbursts of heavy element formation. It has been pointed out (**7**) that overshoot in the negative feedback loop 'grain cooling → solid

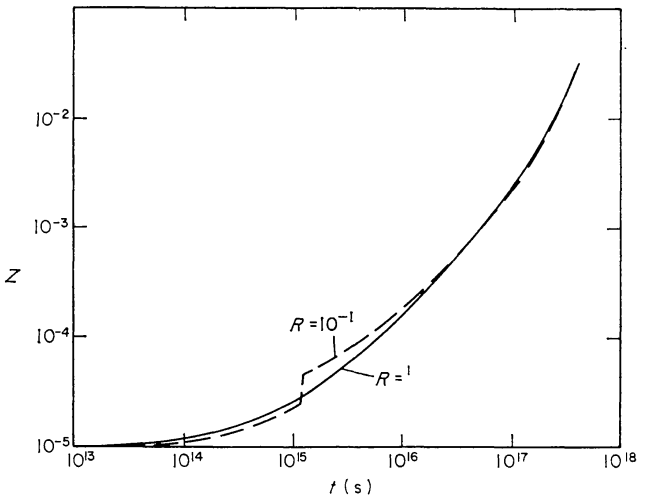

FIG. 8. *Showing how small is the effect, on the growth of heavy element abundances with time, of raising* Z_{SM} *from* 10^{-5} *to* 10^{-3}.

hydrogen condensation → star formation → grain heating' may produce oscillations in the rate of star formation. In the present case it is necessary that this should result also in oscillations in the densities of the interstellar clouds. The evaporation of the solid hydrogen grains by bursts of star formation and the subsequent increase in gas pressure, as described in Section 3, may indeed produce such an effect.

A proper evaluation of such an effect requires a knowledge of the frequency distribution of the densities of the interstellar clouds, which we do not have. It may be noted, however, that the increase in heavy element abundances at each outburst of supernovae would, from Fig. 5(b), be $\sim 10^{-4}$, and that about a hundred oscillations through the ' supernova ' density would be required to raise the heavy element abundance to $\approx 0{\cdot}01$. A hundred such oscillations would occupy a time $\gtrsim 10^{8}$ yr and is therefore at the limit of the time scale set by the frequency of Seyfert galaxies and quasars. The possibility therefore does not appear to be a likely one.

V. C. Reddish:
Royal Observatory, Edinburgh.

N. C. Wickramasinghe:
Institute of Theoretical Astronomy, Cambridge.

REFERENCES

(1) Reddish, V. C., 1965. *Vistas Astr.*, **7**, 173.
(2) Reddish, V. C., 1967. *Mon. Not. R. astr. Soc.*, **135**, 251.
(3) Wickramasinghe, N. C. & Reddish, V. C., 1968. *Nature, Lond.*, **218**, 661.
(4) Garzoli, S. L. & Varsavsky, C. M., 1967. *Astrophys. J.*, **145**, 79.
(5) Kerr, F. J. & Garzoli, S. L., 1968. *Astrophys. J.*, **152**, 51.
(6) Heiles, C., 1967. *Astrophys. J., Suppl. Ser.*, **15**, 97.
(7) Hoyle, F., Reddish, V. C. & Wickramasinghe, N. C., 1968. *Nature, Lond.*, **218**, 1124.
(8) Solomon, P. M. & Wickramasinghe, N. C., 1969. In press.
(9) Krishna Swamy, K. S. & Wickramasinghe, N. C., 1969. *Mon. Not. R. astr. Soc.*, in press.
(10) Kafran-Kassim, M. A., 1961. *Astrophys. J.*, **133**, 821.
(11) Cugnon, P., 1968. *Bull. astr. Insts Neth.*, **19**, 363.
(12) Reddish, V. C., 1968. *Q. Jl R. astr. Soc.*, **9**, 409.
(13) Reddish, V. C., 1962. *Sci. Prog., Oxf.*, **50**, 235.

(14) Hoyle, F. & Fowler, W. A., 1960. *Astrophys. J.*, **132,** 565.
(15) Hoyle, F. & Wickramasinghe, N. C., 1962. *Mon. Not. R. astr. Soc.*, **124, 417.**
(16) Hoyle, F. & Wickramasinghe, N. C., 1968. *Nature, Lond.*, **218,** 1126.
(17) Wagoner, R. V., Fowler, W. A. & Hoyle, F., 1967. *Astrophys. J.*, **148,** 3.
(18) Hoyle, F. & Fowler, W. A., 1963. *Nature, Lond.*, **197,** 533.
(19) Tayler, R. J., 1967. *Q. Jl R. astr. Soc.*, **8,** 313.
(20) Dixon, M. E., 1966. *Mon. Not. R. astr. Soc.*, **131,** 325.
(21) Wood, D. B., 1966. *Astrophys. J.*, **145,** 36.
(22) Field, G. B., 1965. *Astrophys. J.*, **142,** 531.
(23) Pikelner, S. B., 1968. *Soviet Astr.*, **11,** 737.